EFFECT OF VARIABLE ELECTRIC CONDUCTIVITY ON RADIATIVE HEAT TRANSFER FLOW ALONG A VERTICAL PLATE OF MICROPOLAR FLUID WITH VARIABLE HEAT FLUX AND UNIFORM SOURCE (OR SINK) IN A POROUS MEDIA

M. J. Uddin

Department of Natural Science, Daffodil International University, Dhaka
E-mail: jashim@daffodilvarsity.edu.bd

Abstract. *A two-dimensional steady convective flow of a micropolar fluid past a vertical porous flat plate in the presence of radiation with variable heat flux has been analyzed numerically. The local similarity solutions for the flow, velocity profile, microrotation and heat transfer characteristics are illustrated graphically for various parameters entering into the problems. The effects of the pertinent parameters on the local skin friction coefficient, plate couple stress and the heat transfer are also calculated. Effect of variable electric conductivity and constant electric conductivity has been analyzed numerically for the skin friction coefficient and rate of heat transfer. The result shows that for Magnetic field parameter, Prandlt number, temperature dependent heat source (or sink) parameter and space dependent heat source (or sink) parameter, the variable electric conductivity is high pronounced than that of constant electric conductivity for micropolar fluid for both the case of skin friction coefficient and Nusselt number.*

Keywords: *radiation, micropolar fluid, porous medium, locally self-similar solution, heat transfer, electric conductivity.*

1. Introduction

Micropolar fluids are fluids with microstructure belonging to a class of fluids with nonsymmetrical stress sensor referred to as polar fluids. A micropolar fluid is the fluid with interior structures in which coupling between the spin of each particle and the macroscopic velocity field is taken into account [1]. It is a hydrodynamical framework suitable for granular systems which consist of particles with macroscopic size. Many transport processes that occur both in nature and in industries involve fluid flows with combined heat and mass transfer. Such flows are driven by the buoyancy effects arising from the density variations caused by the variations in temperature and/ or species concentrations.

The dynamics of micropolar fluids, originated from the theory of Eringen [2] has been a popular area of research. This theory may be applied to explain the flow of colloidal suspensions (Hadimoto and Tokioka [3]), liquid crystals (Lockwood et al. [4]), polymeric fluids, human and animal blood (Ariman et al. [5]) and many other situations. Ariman et al. [5] have given an excellent review of the micropolar fluid model and its application. Soundalgekar and Takhar [6] studied the flow and heat transfer past a continuously moving plate in a micropolar fluid and also they studied radiation effects on free convection problems involving absorbing emitting fluids. Hoyt and Fabula [7] have shown experimentally that the fluids containing minute polymeric additives can reduce skin-friction by 25-30%. This reduction was explained by the theory of micropolar fluid. Gorla [8] studied mixed convection in a micropolar fluid from a vertical surface with uniform heat flux. Rees and Pop [9] studied free convection boundary layer flow of micropolar fluids from a vertical flat plate while Mohammadein and Gorla [10] studied the same flow bounded by stretching sheet with prescribed wall heat flux, viscous dissipation and internal heat generation. Aissa and Hassanien et al. [11] studied unsteady magnetohydrodynamic micropolar fluid flow and heat transfer over a vertical porous plate through a porousmedium in the presence of thermal and mass diffusion with a constant heat source. Rahman and Sattar [12] studied

Date of submission : 27.08.2012 Date of acceptance : 13.04.2013

magnetohydrodynamic convective flow of a micropolar fluid past a vertical porous plate in the presence of heat generation/absorption.
El-Arabawy [13] studied the effect of suction/injection on a micropolar fluid past a continuously moving plate in the presence of radiation. Rahman and Sattar [14] studied transient convective heat transfer flow of a micropolar fluid past a continuously moving vertical porous plate with time dependent suction in the presence of radiation.
In the present work we investigate the thermal radiation of the boundary layer flow of micropolar fluid past vertical porous plate. Also it has been analyzed the flow of a variable electric conductivity and constant electric conductivity of micropolar fluid with non-uniform heat source and sink over a permeable flat plate subject to a uniform surface heat flux boundary condition.

2. Mathematical formulations

Let us consider a steady two-dimensional flow of an incompressible, viscous micropolar fluid of temperature T_∞ past a heated vertical porous flat plate immersed in a porous medium and there is a suction velocity $v_0(x)$ at the plate. Consider a variable surface heat flux such that the temperature at the surface of the plate is proportional to x^m (x measures the distance from the leading edge along the surface of the plate and m is a constant). The flow is assumed to be in the x-direction, which is taken along the plate in the upward direction and y-axis is normal to it. The flow configuration and the coordinate system are shown in the Fig. 1.

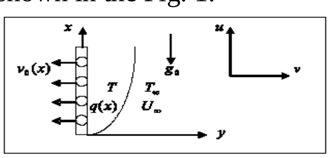

Figure 1: Flow configuration and coordinate system.

Within the framework of the above-noted assumptions, we assume that the Boussinesq and boundary layer approximations hold and using the Darcy-Forchheimer model, the governing equations relevant to the problem in the presence of radiation are given by:
Continuity Equation:

$$\frac{\partial u}{\partial x}+\frac{\partial v}{\partial y}=0, \tag{1}$$

Momentum Equation:

$$u\frac{\partial u}{\partial x}+v\frac{\partial u}{\partial y}=\upsilon_a\frac{\partial^2 u}{\partial y^2}+\frac{S}{\rho}\left(\frac{\partial \sigma}{\partial y}\right)^2+ g_0\beta(T-T_\infty)-\frac{\upsilon_a}{\kappa'}(u-U_\infty) -\frac{b}{\kappa'}(u-U_\infty)^2-\frac{\sigma_0 B_0^2 u^2}{\rho x}, \tag{2}$$

Angular momentum Equation:

$$u\frac{\partial \sigma}{\partial x}+v\frac{\partial \sigma}{\partial y}=\frac{\upsilon_s}{\rho j}\frac{\partial^2 \sigma}{\partial y^2}-\frac{S}{\rho j}\left(2\sigma+\frac{\partial u}{\partial y}\right), \tag{3}$$

Energy Equation:

$$u\frac{\partial T}{\partial x}+v\frac{\partial T}{\partial y}=\frac{k}{\rho c_p}\frac{\partial^2 T}{\partial y^2}-\frac{1}{\rho c_p}\frac{\partial q_r}{\partial y} +\frac{\kappa U_\infty}{2\upsilon_a x\rho c_p}[Q(T-T_\infty)+Q^*(T_w-T_\infty)e^{-\eta}], \tag{4}$$

where u, v are the velocity components along x, y co-ordinates respectively, $\upsilon_a=\frac{\mu+S}{\rho}$ is the kinematic viscosity, ρ is the mass density of the fluid, μ is the coefficient of dynamic viscosity, $\upsilon_s=(\mu+\frac{S}{2})j$ is the microrotation viscosity or spin-gradient viscosity, S is the microrotation coupling coefficient (also known as the coefficient of gyro-viscosity or as the vortex viscosity), σ is the microrotation component normal to the xy-plane, b is the empirical constant, j is the micro-inertia density, T is the temperature of the fluid in the boundary layer, T_∞ is the temperature of the fluid outside the boundary layer, c_p is the specific heat of the fluid at constant pressure, k is the thermal conductivity, g_0 is the acceleration due to gravity, β is the volumetric coefficient of thermal expansion, Q and Q^* are the coefficients of space and temperature dependent heat source/sink respectively.
The corresponding boundary condition for the above problem are given by

$$\left.\begin{aligned} &u=0, v=v_0(x), \sigma=-n\frac{\partial u}{\partial y}, \frac{\partial T}{\partial y}=-\frac{q_w}{\kappa} \text{ at } y=0,\\ &u=U_\infty,\ \sigma=0,\ T=T_\infty \quad \text{as } y\to\infty, \end{aligned}\right\} \tag{5}$$

Positive and negative values for v_0 indicate blowing and suction respectively, while $v_0 = 0$ corresponds to an impermeable plate.

3. Transformation of Model

In order to obtain local similarity solution of the problem we adopted the following non-dimensional variables which have been used by many authors in the literature.

$$\eta = y\sqrt{\frac{U_\infty}{2\upsilon_a x}}\,, \psi = \sqrt{2\upsilon_a U_\infty x}\, f(\eta)\,,$$

$$\sigma = \sqrt{\frac{U_\infty^3}{2\upsilon_a x}}\, g\,,\ T - T_\infty = \theta(\eta) T^* \qquad (6)$$

Where ψ is the stream function, U_∞ is some reference velocity and

$$T^* = \sqrt{\frac{2\upsilon_a x}{U_\infty}}\ (\frac{q_w}{k})\,.$$

Since $u = \frac{\partial \psi}{\partial y}$ and $v = -\frac{\partial \psi}{\partial x}$ we have from equation that,

$$u = U_\infty f' \text{ and } v = -\sqrt{\frac{\upsilon_a U_\infty}{2x}}(f - \eta f'). \qquad (7)$$

Here f is non-dimensional stream function and prime denotes differentiation with respect to η.

Now introducing equation (6) and (7) into equations (2)-(4), we obtain

$$f''' + ff'' + K(g')^2 + 2\gamma\theta - 2\lambda(f'-1) - Fs(f'-1)^2 - Mf'^2 = 0 \qquad (8)$$

$$G_2 g'' - 2G_1(2g + f'') + (f'g + g'f) = 0 \qquad (9)$$

$$\theta'' + Pn(f\theta' - 5f'\theta) + \Pr(f\theta' - f'\theta) + Q\theta + Q^* e^{-\eta} = 0 \qquad (10)$$

where $K = \frac{S}{\rho\upsilon_a}$ is the coupling parameter, $\gamma = \left(\frac{2Gr_x^2}{\mathrm{Re}_x}\right)^{\frac{1}{2}}$ is the local buoyancy parameter, $Gr_x = \frac{g_0 \beta b_0 x^4}{\kappa U_\infty^2}$ is the modified Grashof number $\mathrm{Re}_x = \frac{U_\infty x}{\upsilon_a}$ is the local Reynolds number, $\lambda = \frac{1}{D_a}$ is the Darcy parameter, $D_a = \frac{K' U_\infty x}{\upsilon_a x}$ is the modified Darcy number, $F_s = \frac{bx}{K'}$ is the modified Forchheimer number, $G_1 = \frac{S_x}{\rho j U_\infty}$ is the vortex viscosity parameter, $G_2 = \frac{\upsilon_s}{\rho j \upsilon_a}$ is the spin gradient viscosity parameter, $Pn = \frac{3N\,\Pr}{3N+4}$ is the radiative Prandtl number, $N = \frac{\kappa\kappa_1}{4\sigma_1 T_\infty^3}$ is the radiation parameter, $\Pr = \frac{\rho \upsilon_a c_p}{\kappa}$ is the Prandtl number, $M = \frac{2\sigma_0 B_0^2}{\rho}$ is the magnetic field parameter.

Then the corresponding boundary conditions (5) become,

$$\left.\begin{aligned} &f = V_0,\ f' = 0,\ g = -nf'',\ \theta' = -1 \ \text{ at } \eta = 0, \\ &f' = 1,\ g = 0,\ \theta = 0 \qquad \text{as } \eta \to \infty. \end{aligned}\right\} \qquad (11)$$

where $V_0 = -v_0\sqrt{\frac{2x}{\upsilon_a U_\infty}}$ is the suction velocity at the plate for $V_0 > 0$.

4. Skin friction coefficient, plate couple stress and Nusselt number

The quantities of chief physical interest are the skin-friction coefficient, plate couple stress and the Nusselt number (rate of heat transfer). The equation defining the wall shear stress is

$$\tau_w = (\mu + S)(\frac{\partial u}{\partial y})_{y=0} + S(\sigma)_{y=0}\,. \qquad (12)$$

The local skin-friction coefficient is defined as

$$C_f = \frac{\tau_w}{\frac{1}{2}\rho U_\infty^{\ 2}} = (2\,\mathrm{Re}_x^{\ -1})^{\frac{1}{2}}[f''(0) + K_g(0)] = (2\,\mathrm{Re}_x^{-1})^{\frac{1}{2}}(1 - nK) f''(0) \qquad (13)$$

Thus from equation (13) we see that the local values of the skin-friction coefficient C_f is proportional to $f''(0)$.

The equation defying the plate couple stress is

$$M_w = \upsilon_s \left(\frac{\partial \sigma}{\partial y}\right)_{y=0} \tag{14}$$

The dimensionless couple stress is defined by

$$M_x = \frac{M_w}{\frac{1}{2}\rho \upsilon_a U_\infty} = \frac{G_2 K}{G_1} g'(0) \tag{15}$$

Thus the local plate couple stress in the boundary layer is proportional to $g'(0)$. We may define a non-dimensional coefficient of heat transfer, which is known as Nusselt number as follows:

$$Nu_x = \frac{x\,h(x)}{k}, \tag{16}$$

Where $h(x) = \dfrac{q_w(x)}{T_w - T_\infty}$ and $q_w(x) = -\kappa \left(\dfrac{\partial \sigma}{\partial y}\right)_{y=0} - \dfrac{4\sigma_1}{3\kappa_1}\left(\dfrac{\partial T^4}{\partial y}\right)_{y=0}$ is the quantity of heat transferred through the unit area .Now the rate of heat transfer, in terms of the dimensionless Nusselt number, given by

$$Nu_x = (2^{-1}\,\mathrm{Re}_x)^{\frac{1}{2}} \frac{1}{\theta(0)}. \tag{17}$$

Thus from equation (16) we see that the local Nusselt number Nu_x is reciprocal to θ_0. Hence the numerical values proportional to C_f, M_x and Nu_x are calculated from equations (13), (14) and (16) are shown in Figures 3-8.

5. Numerical Solutions

The set of equations (8)–(10) is highly nonlinear and coupled and therefore the system cannot be solved analytically. The nonlinear systems (8)–(10) with boundary conditions (11) are solved using the Nachtsheim and Swigert [15] shooting iteration technique.

5.1. Code verification

In order to verify the effects of the step size $\Delta\eta$ we established the code for our model with three different step sizes as $\Delta\eta = 0.001, \Delta\eta = 0.003$, and $\Delta\eta = 0.005$ and in each case we found excellent agreement among them. Figures 2(a)-(c), respectively, shows the velocity, microrotation, and temperature profiles for different step sizes. The results for the three different step sizes are graphically indistinguishable. Throughout the calculations we have fixed the value of $\Delta\eta = 0.001$ as the solutions are independent of step sizes.

a.

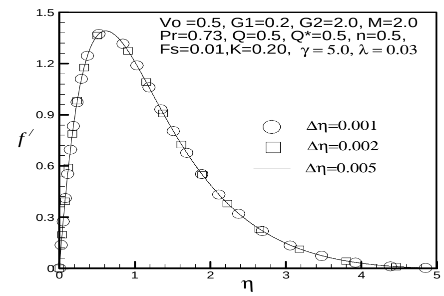

b.

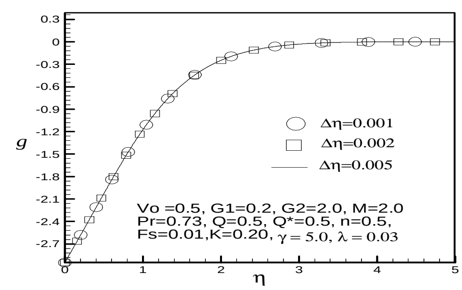

c.

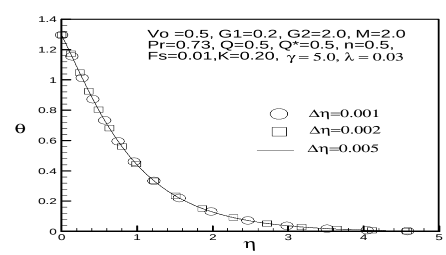

Figure 2: (a) Velocity, (b) microrotation and (c) temperature profiles for different values of $\Delta\eta$.

6. Result and discussion

Fig. 3(a)–(c), 4(a)-(c), 5(a)-(c),6(a)-(c), 7(a)–(c) and 8(a)–(c) respectively, represents the velocity, microrotation and temperature profiles for different values of V_0, G_1, M, Pr, Q and Q^* and n . From Fig. 3(a) we note that the velocity decreases with the increase of the suction parameter indicating that the suction tends to retard the convective motion of the fluid.

It can also be seen that for cooling of the plate the velocity profiles decrease monotonically with increase of suction parameter indicating the usual fact that suction stabilizes the boundary layer growth. This effect is stronger near the surface of the plate. From Fig. 3(b) we see that very close to the plate $\eta \leq 0.4$, microrotation increases with the increase of the suction parameter. As we move away from the plate, the effect of V_0 becomes more pronounced. Fig. 3(c) reveals that the temperature in the thermal boundary layer decreases with the increase of V_0. This is due to the fact that suction tends to speed up the velocity field, which in turn reduces the heat transfer. This is manifested with higher temperatures in the thermal boundary layer.

Fig. 4(a) shows the effect of vortex viscosity parameter G1 on the velocity profiles for cooling plate. From here we see minor decreasing effect of G1 on the velocity profiles. Fig. 4(b) shows the effect of G1 on the microrotation profiles. From this figure we see that microrotation increases very rapidly with the increase of the vortex viscosity parameter G1. It is also understood that as the vortex viscosity increases the rotation of the micropolar constituents gets induced in most part of the boundary layer except very close to the wall where kinematic viscosity prevails the flow. From Fig. 4(c) we found slight effect of G1 on temperature profiles.

From Fig. 5(a) we note that the velocity decreases with the increase of the magnetic field parameter indicating that the magnetic field tends to retard the convective motion of the fluid. This effect is stronger near the surface of the plate. From Fig. 5(b) we see that very close to the plate $\eta \leq 1$, microrotation increases with the increase of the magnetic field parameter. As we move away from the plate, the effect of M becomes less pronounced. Fig. 5(c) reveals that the temperature in the thermal boundary layer increases with the increase of M. This is due to the fact that the magnetic field tends to retard the velocity field, which in turn reduces the heat transfer. This is manifested with higher temperatures in the thermal boundary layer. These results clearly demonstrate that the magnetic field can be used as a means of controlling the flow and heat transfer characteristics.

Fig. 6(a) shows the velocity profiles for different values of Prandtl number Pr for a cooled plate. As the Prandtl number increases, viscous forces tend to suppress the buoyancy forces and cause the velocity in the hydrodynamic boundary layer to decrease. For small Pr, the boundary layer is thick. For large Pr values the velocity is found to decrease monotonically and the boundary layer thickness is seen to decrease. Fig. 6(b) shows the microrotation profiles for the various values of the Prandtl number Pr. From this figure it can be seen that when the plate is cooled, microrotation increases with the increase in Prandtl number. It is also observed that away from the plate $\eta \leq 2$ these profiles overlap. Fig. 6(c) reveals the effects of the Prandtl number on the thermal boundary layer are similar to those found in the hydrodynamic boundary layer.

Fig. 7(a) it is observed that when the heat is generated (Q,Q* > 0) the buoyancy force increases giving rise to higher velocities in the boundary layer. Fig. 7(b) shows that as Q and Q* increases, the microrotation decreases. When heat generation occurs in the fluid, one would expect the temperature in the thermal boundary layer to increase. This corroborated by Fig. 7(c) where it is seen that the temperatures do indeed increase as Q and Q* increases.

From the fig 8(a)-(c), it can be observe that the velocity profile raised, microrotation profile and temperature profile are decreased as n increased. It can be also observed that the flow is more vigorous in a strongly concentrated micropolar fluid compared with the flow in a weakly concentrated micropolar fluid.

In Table 1 presents skin-friction coefficient and rate of heat transfer of micropolar fluid for various values of the magnetic field parameter for the cases of variable fluid electric conductivity (VEC) as well as of constant fluid electric conductivity (CEC). From this table it is clear that both the skin-friction and heat transfer rate are higher for the case of VEC than for the CEC for the micropolar fluid.

In Table 2 presents skin-friction coefficient and rate of heat transfer of micropolar fluid for various values of the temperature dependent heat source (or sink) parameter (Q) and space dependent heat source (or sink) parameter (Q*) for the cases of variable fluid electric conductivity (VEC) as well as of constant fluid electric conductivity (CEC). This table shows that skin-friction coefficients and heat transfer rate corresponding to VEC case are higher than those of CEC for all increasing values of Q and Q*. When Q* increases from 0 to 1 skin-friction coefficient for micropolar fluid increases by 91% (for the case of VEC) and 81.12% (for the case of CEC) while for similar increase of Q the corresponding change in skin-friction coefficient is 8.13% (for case of VEC) and 9.29% (for the case of CEC). Table 2 also depicts that rate of heat transfer from the inclined surface to the micropolar fluid reduces

Table1 Values of c_f^* and Nu_x^* for various values of M

M	c_f^*		Nu_x^*	
	VEC	CEC	VEC	CEC
0.0	4.7636	4.7636	2.8641	2.8641
0.5	4.5957	4.5361	2.8225	2.8048
1.0	4.4709	4.3260	2.7897	2.7550
1.5	4.3724	4.2005	2.7627	2.7161
2.0	4.2915	4.0941	2.7397	2.6821
2.5	4.2231	4.0030	2.7197	2.6519
3.0	4.1638	3.9226	2.7021	2.6248
3.5	4.1117	3.8508	2.6862	2.6002

by 6.13% (for the case of VEC) and 6.22% (for

Table 2 Values of c_f^* and Nu_x^* for various values of Q and Q^*

Q	Q^*	c_f^*		Nu_x^*	
		(VEC)	(CEC)	(VEC)	(CEC)
0.5	0.0	2.9238	2.7155	3.3035	3.2392
0.5	0.2	3.5291	3.3427	3.0390	2.9691
0.5	0.5	4.2915	4.0941	2.7397	2.6821
0.5	0.8	4.9162	4.7488	2.5121	2.4689
0.5	1.0	5.2955	5.1855	2.3868	2.3522
0.0	0.5	4.1288	3.9179	2.8262	2.7683
0.2	0.5	4.1927	3.9871	2.7917	2.7338
0.5	0.5	4.2915	4.0941	2.7397	2.6821
0.8	0.5	4.3940	4.2057	2.6876	2.6304
1.0	0.5	4.4644	4.2820	2.6529	2.5960

the case of CEC) when Q increases from 0 to 1 whereas this reduction is 27.75% (for the case of VEC) and 27.38% (for the case of CEC) when Q* increases from 0 to 1. This table clearly demonstrates that rate of heat transfer strongly depends on the temperature dependent heat source parameter less than the space dependent heat source parameter. The opposite effect observed for the case of heat absorption.

Table 3 illustrates the skin friction coefficient and rate of heat transfer for various values of Prandtl number Pr for the case of VEC and CEC. From this table it can be said that VEC is higher than CEC for both the skin friction coefficient and rate of heat transfer. Moreover, in the case of skin friction coefficient, VEC as well as CEC both decreases as different values of Pr increases but the reverse can be found for the rate of heat transfer.

Table 4 shows that the skin friction coefficient and rate of heat transfer for various values of Radiative Prandtl number Pn for the case of VEC and CEC. The skin friction coefficient decreases 82.84 % (for the case of VEC) and 86.21% (for the case of CEC) and rate of heat transfer increases 281% (for the case of VEC) and 240% (for the case of CEC) as Pn increases from 0 to 2. From this table we found that the substantial effect of radiative Prandtl number on skin friction coefficient and rate of heat

Table 3 Values of c_f^* and Nu_x^* for various values of Pr

Pr	c_f^*		Nu_x^*	
	(VEC)	(CEC)	(VEC)	(CEC)
0.0	4.9434	4.7706	2.4602	2.4183
0.73	4.2915	4.0941	2.7397	2.6821
1.0	4.0936	3.8911	2.8397	2.7767
1.5	3.7722	3.5627	3.0214	2.9492
2.0	3.4977	3.2840	3.1998	3.1190
2.97	3.0633	2.8464	3.5398	3.4438
4.24	2.6308	2.4145	3.9783	3.8647
7.0	2.0021	1.7948	4.9243	4.7778

transfer for both VEC and CEC.

Table 4 Values of c_f^* and Nu_x^* for various values of Pn

P_n	c_f^*		Nu_x^*	
	VEC	CEC	VEC	CEC
0.0	13.9461	15.6648	1.1362	1.2414
0.2	9.6262	9.9737	1.4907	1.5285
0.5	6.6299	6.5818	1.9691	1.9587
0.73	5.3252	5.1793	2.3236	2.2885
1.0	4.2915	4.0941	2.7397	2.6821
1.5	3.1019	2.8731	3.5236	3.4351
2.0	2.3930	2.1601	4.3287	4.2172

a.

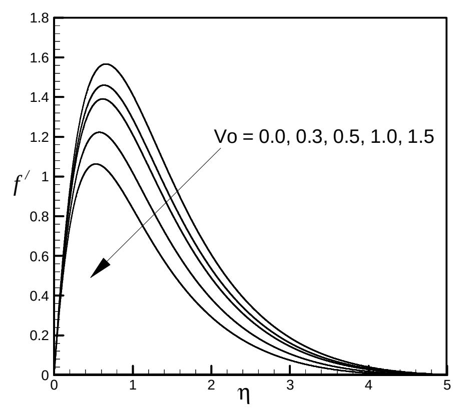

b.

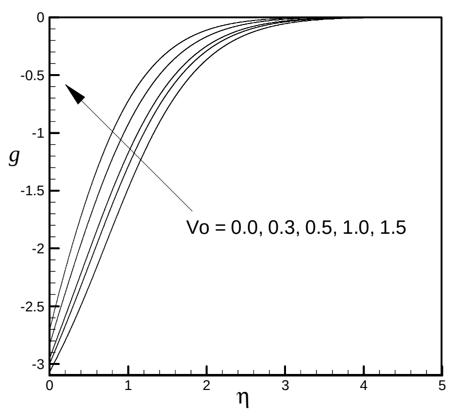

c.

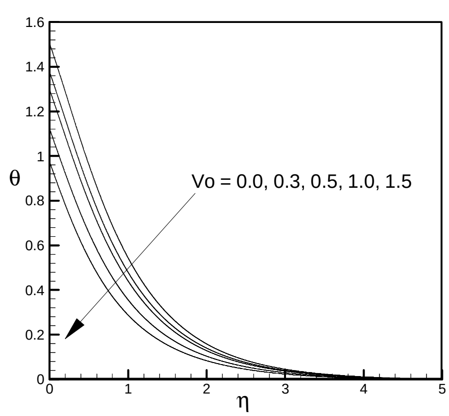

Figure 3: (a)Velocity,(b) Microrotation, and (c)Temperature profiles for different values of suction parameter V_0

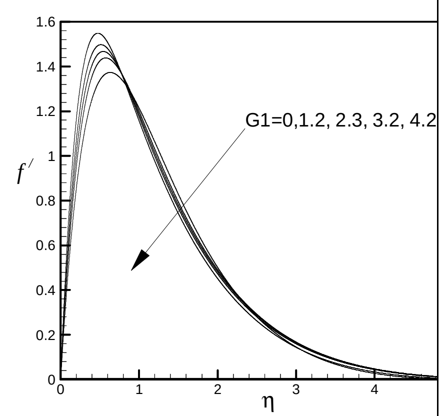

b.

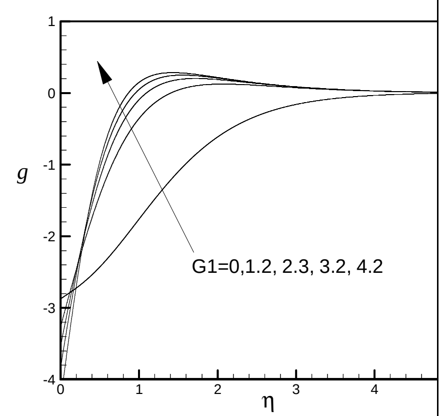

c.

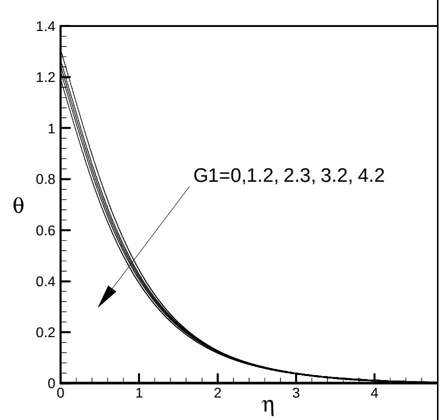

Figure 4: (a)Velocity,(b) Microrotation, and (c)Temperature profiles for different values of G_1

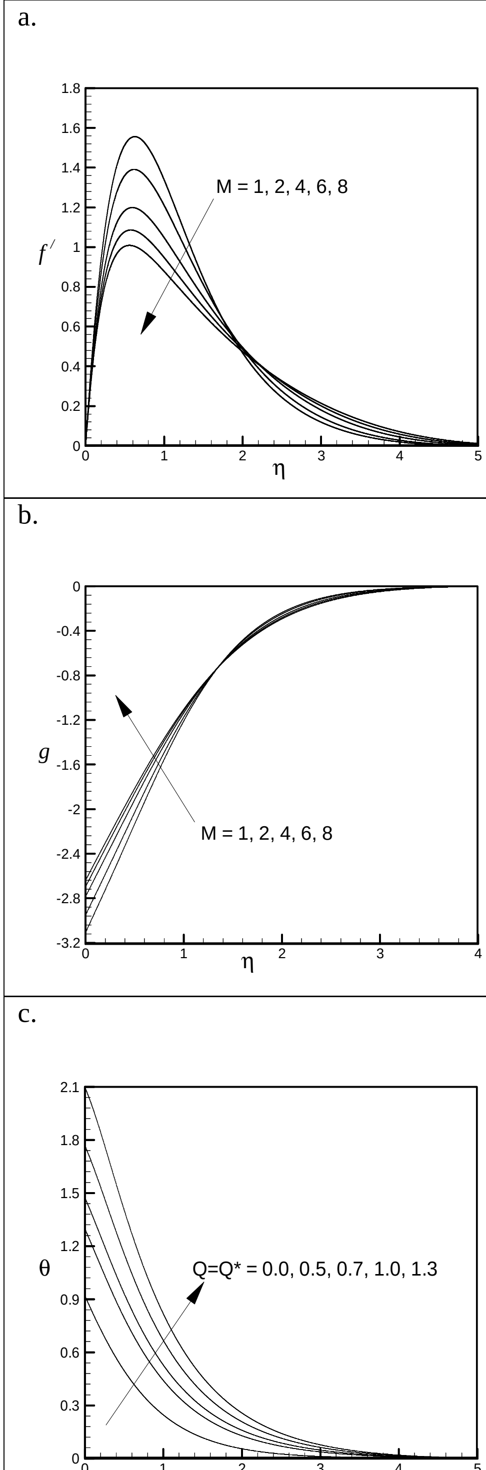

Figure 5: Variations of non dimensional (a)Velocity,(b) Microrotation, and (c)Temperature profiles for different values of M

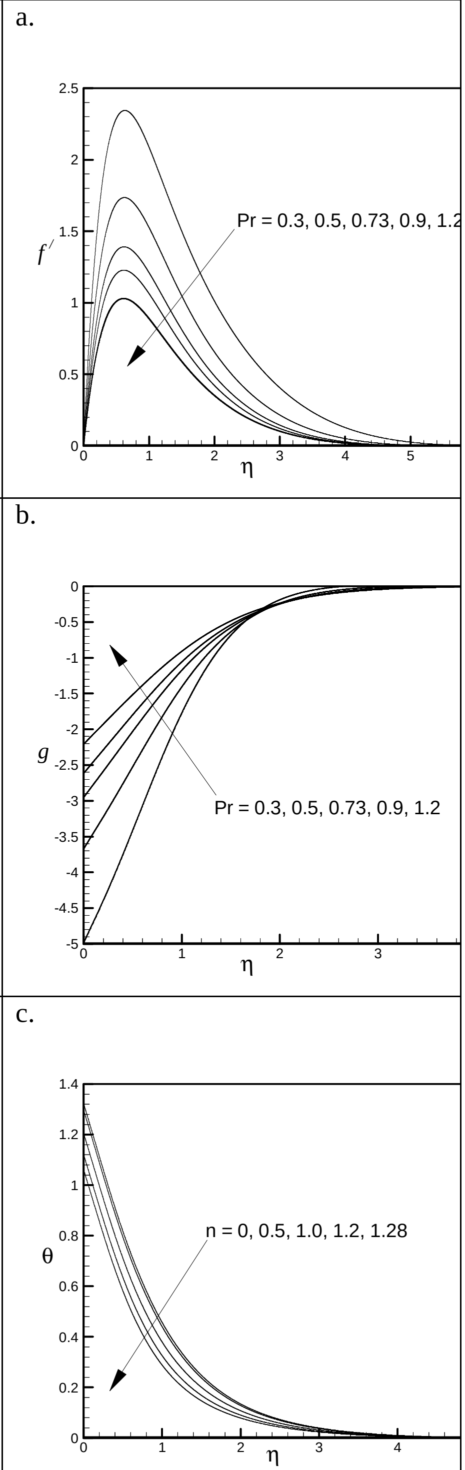

Figure 6: Variations of non dimensional (a)Velocity,(b) Microrotation, and (c)Temperature profiles for different values of Pr

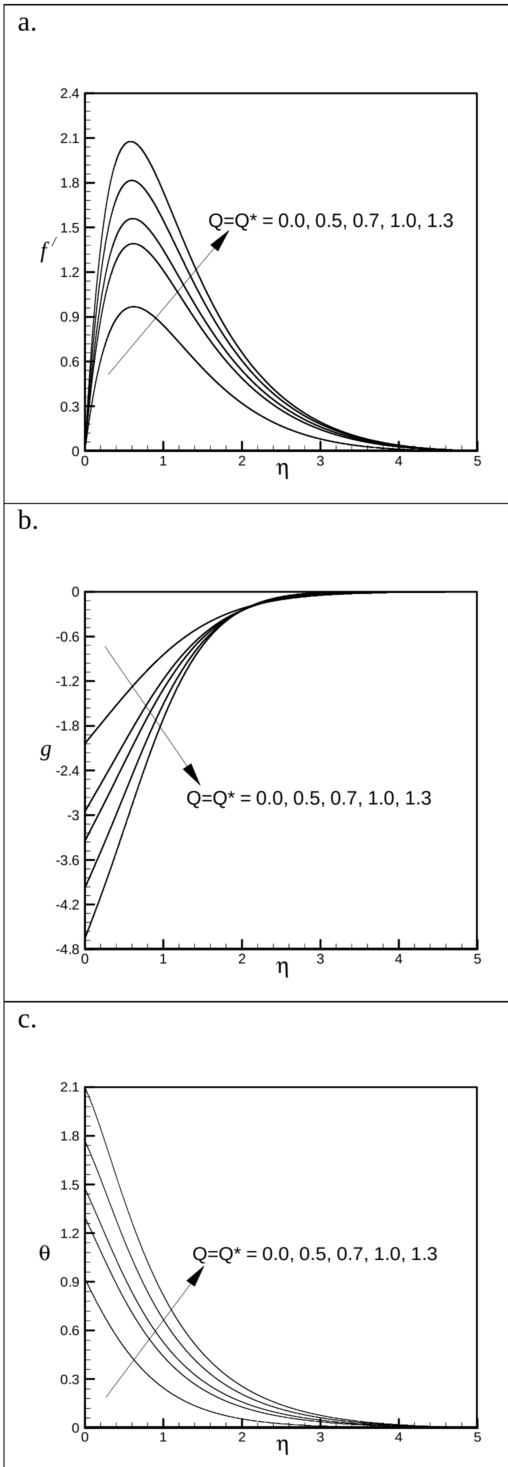

Figure 7: Variations of non dimensional (a)Velocity,(b) Microrotation, and (c)Temperature profiles for different values of $Q\ und\ Q^*$

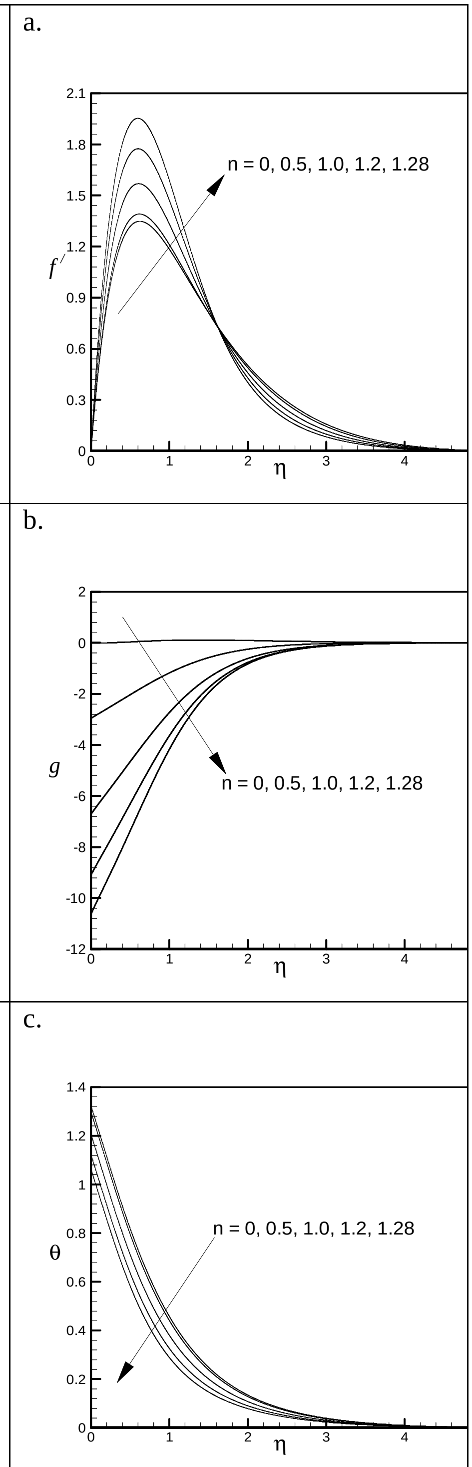

Figure 8: Variations of non dimensional (a)Velocity,(b) Microrotation, and (c)Temperature profiles for different values of n

7. Conclusion

In this paper, we have investigated numerically the effect of variable electric conductivity on radiative heat transfer flow of micropolar fluid past a vertical permeable flat plat. The following conclusions can be drawn as a result of the numerical computations:

1. Velocity profile increases with the increase of the temperature dependent heat source (or sink) parameter (Q) and space dependent heat source (or sink) parameter(Q^{*}), microrotation parameter and decreases with the increase of suction parameter, Prandtl number, magnetic field parameter, vortex viscosity parameter.
2. Plate couple stress increases with the increase of suction parameter, vortex viscosity parameter, magnetic field parameter, Prandtl number where as decreases with the increase of heat source(or sink) parameter, microrotation parameter.
3. The rate of heat transfer increases with the increase of Magnetic field parameter, heat source(or sink) parameter but decreases with the increase of the suction parameter, viscosity parameter, Prandtl number, microrotation parameter.
4. Skin friction coefficient increases with the increases of heat source (or sink) parameter and decreases with increase of Magnetic field parameter, Prandtl number, radiative prandtl number for both the cases of CEC and VEC.
5. Nusselt number decreases with increase of Magnetic field parameter and heat source(or sink) and decreases with the increase of prandtl number, radiative parandtl number for both the case of VEC and CEC

Acknowledgement

I would like to express gratitude the anonymous referees for their very expertise remarks for the further enhancement of the work.

8. References

1. M.M. Rahman, T. Sultana, Radiative Heat Transfer Flow of Micropolar Fluid withVariable Heat Flux in a Porous Medium
2. A.C. Eringen, Theory of micropolar fluids, J. Math. Mech., 16, pp. 1–18, 1966.
3. B. Hadimoto, T. Tokioka, Two-dimensional shear flows of linear micropolar fluids, Int. J. Engi Sci., 7, pp. 515–522, 1969.
4. F. Lockwood, M. Benchaitra, S. Friberg, Study of polyotropic liquid crystals in viscometric flow and clastohydrodynamic contact ASLE Tribology Trans., 30, pp. 539–548, 1987.
5. T. Ariman, M.A. Turk, N.D. Sylvester, Microcontinuum fluid mechanics – a review, Int. J. Eng. Sci., 12, pp. 273–293, 1974.
6. V.M. Soundalgekar, H. S. Takhar, Flow of a micropolar fluid on a continuous moving plat, Int. J. Eng. Sci., 21, p. 961, 1983.
7. J.W. Hoyt, A.G. Fabula, The Effect of Additives on Fluid Friction, US Naval Ordinance Test Station Report, 1964
8. R. S.R. Gorla, Mixed convection in a micropolar fluid from a vertical surface with uniform heat flux, Int. J. Engi. Sci., 30, pp. 349–358, 1992.
9. D.A. S. Rees, I. Pop, Free convection boundary layer flow of micropolar fluid from a vertical flat plat, IMA J. Appl. Math., 61, pp. 179–197, 1998.
10. A.A. Mohammadein, R. S.R. Gorla, Heat transfer in a micropolar fluid over a stretching sheet with viscous dissipation and internal heat generation, Int. J. Num. Meth., Heat Fluid Flow., 11(1), pp. 50–58, 2001.
11. I.A. Hassanien, F. S. Ibrahim, A.A. Bakr,Unsteady magnetohydrodynamic micropolar fluid flow and heat transfer over a vertical porous plate through a porous medium in the presence of thermal and mass diffusion with a constant heat source, Canadian J. Phys., 82(10), pp. 775–790, 2004.
12. M.M. Rahman, M.A. Sattar, Magneto hydrodynamic convective flow of a micropolar fluid past a continuously moving vertical porous plate in the presence of heat generation/absorption, ASME J. H. Transfer, 128, pp. 142–152, 2006.
13. H.A.M. El-Arabawy, Effect of suction/injection on the flow of a micropolar fluid past aContinuously moving plate in the presence of radiation, Int. J. Heat Mass Transfer, 46, pp. 1471–1477, 2003.
14. M.M. Rahman, M.A. Sattar, Transient convective flow of micropolar fluid past a continuously moving vertical porous plate in the presence of radiation, Int. J. App. Mech. Engi., 12(2), pp. 497–513, 2007.
15. P.R. Nachtsheim, P. Swigert, Satisfaction of the asymptotic boundary conditions in numerical solution of the system of non-linear equations of boundary layer type, NASSA TND-3004, 1965.